# DFT and Monte Carlo study of the W(001) surface reconstruction

**I. N. Yakovkin[1]*, I. I. Yakovkin[2], N. V. Petrova[1]**

[1] *Institute of Physics, National Academy of Sciences of Ukraine, Prospect Nauki 46, Kiev, Ukraine*

[2] *Faculty of Physics, Taras Shevchenko National University, Volodymyrska 64/13, Kiev, Ukraine*

The driving force for the W(001) surface reconstruction and electronic structures of pristine and H-covered W(001) surfaces are studied by means of relativistic DFT calculations. The spin-orbit coupling leads to the splitting of the bands. Adsorbed physical monolayer of hydrogen due to forming adsorption bonds stabilizes the (1×1) structure of the H/W(001) surface. The performed calculations have not revealed any substantial nesting of Fermi surface, so do not support the Peierls-like charge-density-wave mechanism of the surface reconstruction. The total energy of the (√2×√2)R45º W(001) surface structure is found to be lower, by 0.14 eV per atom, than for the (1×1) W(001). The dependence of the relative intensity of the characteristic LEED reflection on temperature, obtained with the help of Monte Carlo simulations using the interaction energies estimated from DFT calculations, is in good agreement with available experimental data, thus supporting the concept of the order-disorder type of the transition between the low-temperature (√2×√2)R45º and room-temperature (1×1) surface structures of W(001).

***Keywords:*** Surface reconstruction; W(001); Density functional calculations; Monte Carlo simulations

PACS: 68.35.B; 68.35.Rh; 73.20.-r

* Corresponding author. Email: yakov@iop.kiev.ua

## 1. Introduction

It is well established that in some cases a surface has a lower symmetry than that expected from a simple termination of the bulk crystal. This phenomenon is called the surface reconstruction, which should be distinguished from a more common surface relaxation, that is a variation of the interlayer spacing at the surface without changing the symmetry within the surface plane. The first observation of a prototypical surface reconstruction of W(001) on cooling below room temperature was reported in 1971 by Yonehara and Schmidt [1] in their LEED study of hydrogen adsorption on this surface. Specifically, it was found that a clean W(001) surface, having a (1×1) structure at room temperature, at low temperatures reconstructs into a c(2×2) structure (or, in the other notations, (√2×√2)R45º structure, which might be considered more rigorous since the surface unit cell contains 2 atoms).

In 1977, the observation of the phase transition was confirmed by Felter *et al.* [2] and independently by Debe and King [3]. However, the suggested surface unit cells for the c(2×2) structure were different. In particular, while Yonehara and Schmidt [1] proposed a lateral displacements of surface atoms in the [100] direction (so that they were arranged in couples), Felter *et al.* [2] suggested an alternating displacement of the atoms perpendicular to the surface. Melmed *et al*. and Tung *et al*. [4] observed the occurrence of preferential field evaporation of alternate surface atoms, and thus concluded that W(001) is reconstructed with alternating vertical displacements of the surface atoms from 15 to 580 K. Debe and King [3], in turn, argued that the c(2×2) structure is formed by the lateral shift of surface W atoms in the [110] direction to form parallel zig-zag chains, so that the symmetry of the low-temperature phase is *p2mg* [5]. The W(001) surface undergoes the phase transition to (1×1) at ~220 K [5]. This model of the c(2×2) surface structure of W(001), i.e., zigzag chains of atoms oriented along the [110] azimuthal direction, was further supported in a number of *IV*-LEED studies [5-10].

Hence, the local geometric arrangement of the surface atoms, forming the (√2×√2)R45º structure of W(001), was well established. On the other hand, the driving force for the reconstruction was widely debated. In 1978, following earlier suggestions, Tosatti [11] discussed the Peierls-type two-dimensional (2D) surface charge-density waves (CDW) mechanism of the phase transition. Then there was a long-standing controversy whether the phase transitions on the (001) surfaces of W and Mo may be considered as CDW-transitions or not (see [12-14] for review). It was proposed that the transition from a high-temperature normal-metal state to a low-temperature CDW state that results in the surface reconstruction is continuous, i.e. the second order phase transition, caused by a softening of phonons upon cooling down from $T > T_c$ to $T < T_c$ [12-16]. It was suggested then that the lattice distortion induces the potential $V(q)$ for electrons, according to which the electron charge density is temporally modulated. The charge density modulation would, in turn, weaken the restoration force of the lattice.

The singularity of the susceptibility $\chi(q)$ at $q = 2k_F$ suggests that the effect is most pronounced at $q = 2k_F$. The phonon frequency, $\omega$, of the softened mode is reduced with decreasing temperature. Within the mean-field theory, the temperature at which $\omega = 0$ is achieved corresponds to the transition temperature $T_c$ [15,16].

The Peierls instability is induced by strong electron-phonon interactions, enhanced by so-called "nesting" – overlap of parts of the Fermi surface as a result of a translation $q = 2k_F$. For a single one-dimensional metallic chain of atoms, the Fermi surface consists of two points $k = +k_F$ and $k = -k_F$, which results in a perfect nesting and thus leads to instability of the chain. In 2D case the Peierls-type instability can appear also due to a good nesting in the proper direction, which implies existence of flat segments of the Fermi surface normal to that direction on the surface. (We would like to note in this regard that such flat segments of Fermi surface indeed were found in high-resolution angle-resolved ultraviolet photoelectron spectroscopy (UPES) and DFT calculations for the Mo(112) [17,18] and W(112) [19] surfaces, having a strongly anisotropic relief. With the obtained results and, in particular, wave vector $q = 2k_F$, it was possible to explain the formation of long-period chain structures by the indirect lateral interaction, which is closely related to Friedel oscillations of the electron density). However, a detailed UPES study of the W(001) surface Fermi contours, performed by Campuzano *et al*. [20,21], had shown a pronounced curvature of the Fermi contours just in the [110] direction, which indicated a quite poor nesting, insufficient to produce the necessary singularity in the electronic susceptibility to drive the reconstruction, and therefore the CDW mechanism for the W(001) surface reconstruction was suggested irrelevant.

The transparent picture of electronically driven Peierls-like transition, however, was questioned [12-14,22]. In particular, it was suggested that the instability of the structure is controlled by a real part of susceptibility, which must diverge at $q = 2k_F$ to make CDW mechanism efficient. In real systems, however, the real part (in distinction with imaginary part) never diverge, and therefore a "pure" (Peierls-like) CDW mechanism of the phase transition may be ruled out. It should be noted that the nesting itself is insufficient for a surface reconstruction [12,22]. In any realistic system, the susceptibility does not diverge but has a peak of the real part at $q = 2k_F$, so that the related charge density wave (CDW) can only facilitate the structural transformation (due to electron-phonon coupling), but cannot be a driving force for reconstruction [12,22]. Indeed, an essential prerequisite for the stability of a low-temperature phase, which results from the Peierls-like transition, is a freezing of all phonons that could initiate the backward transition to the structure, pertinent to a high-temperature phase. In the Peierls picture, lattice distortion is a secondary effect that arises in response to an electronically driven charge redistribution that would occur regardless of whether or not the ions

subsequently shift from their high symmetry positions. In real materials, the electronic and ionic instabilities always occur simultaneously [12-14,22].

An alternative explanation of the surface reconstruction of W(001) and Mo(001) surfaces was proposed by Inglesfield [23] and, in somewhat different terms (involving short-range Jahn-Teller-like forces), by Terakura *et al*. [24] and Roelofs and Ying [25]. Thus, Inglesfield [23] suggested that the ideal (1×1) (001) surfaces of Mo and W are inherently unstable, regardless of surface states. The surface atoms want to move sideways to increase their interaction with their nearest neighbours in the substrate, which is just a local bonding effect. It was concluded that the W(001) surface is unstable for arbitrary atomic displacements, with the surface states marginally favoring the displacement which couples them together. The surface atoms then move in an anharmonic potential and the phonon frequencies are temperature dependent, the mode with the coupling wave vector going soft first and giving the observed phase transition.

The surface band structure of W(001) was studied by means of first-principles calculations by several groups [26-28]. The most important results of these calculations are revealed bands of surface resonances crossing $E_F$ (also in the $\Gamma - M$ direction in BZ, that is the [110] crystallographic direction), which were believed to be supporting the Peierls-like models of surface reconstruction. Moreover, the CDW model was seemingly reanimated by more recent UPES studies [29,30]. In particular, in contrast to earlier results [20,21], it was found that the Fermi surface of W(001) has substantial flat parts just in the [110] direction of the surface Brillouin zone (BZ). Similar (and even more detailed) results were obtained also for Mo(001) surface [31-33]. It was concluded, basing on the UPES, that the Fermi surface changes its shape with temperature and its segments normal to the [110] direction become perfectly flat just at the transition temperature $T_c$. It should be noted, however, that these results were obtained in early eighties, and the energy resolution of UPES in [29,30] did not allow for reliable estimates of the shape of Fermi surfaces.

The Jahn-Teller-like short-range interaction model, in turn, was supported by DFT calculations of the changes of total energies of the surface caused by relaxation [34-37]. Thus, Singh and Krakauer [34] performed a*b initio* calculations of the energies related to distortions of the ideal W(001) surface and found that this surface is highly unstable against distortions which reduce the surface-atom spacings. It was proposed that the instability of the ideal surface can be understood in terms of a local model in which the unreconstructed surface is unstable against distortions which increase the effective coordination numbers of the surface atoms. The obtained results were consistent with a locally liquid-like disordered high-*T* phase. Yu *et al*. [35] studied the multilayer reconstruction of the W(001) surface at low temperature and the multilayer relaxation of the unreconstructed surface are investigated using

first-principles total-energy and force calculations. The fully relaxed ideal surface was determined to be unstable by 110 meV per surface atom, which supports the conclusion that the high-temperature phase is disordered. The lateral displacement of the second-layer atoms is about 18% that of the first-layer atoms and the first interlayer distance is contracted by about 6% from the bulk value in the reconstructed surface. Fu *et al*. [36] studied the W(001) structural phase transition by all-electron, frozen-phonon, total-energy calculations and suggested that the strong coupling between surface states and the $M_5$ phonons plays a decisive role in favoring the reconstructed c(2×2) structure with a lateral (110) zig-zag displacement of 0.18 ±0.01 Å and no interlayer relaxation. Han and Ying [37] studied the structural phase transition on W(001) through Monte Carlo simulations of two-dimensional model Hamiltonians and confirmed that the transition is of an order-disorder nature.

For a long time, it has been known that adsorbed hydrogen stabilizes the W(001) surface structure. It is interesting to note that adsorption and diffusion of H on W(001) and in the bulk W was first studied even earlier than the reconstruction of a clean W(001) surface [38-41]. It is well established that hydrogen on W adsorbs dissociatively [41,42] while its diffusion into the bulk is negligible. A saturation H coverage on W(001) (the "physical monolayer") is $\theta = 2.0$, so that the concentration of H atoms is twice that of the substrate. Hydrogen monolayer stabilizes the (1×1) surface structure, so that it does not reconstruct with decreasing temperature. At $\theta = 0.5$, which is 1/4 of the saturation coverage, the surface has a c(2×2) structure (either below or above room temperature), as follows from the corresponding LEED pattern. (It should be noted in this regard that it has been a continuous discussion concerning the origin of the c(2×2) LEED pattern – whether it is produced by adsorbed H atoms, which are believed to have a small cross section for electron diffraction, or stems from the H-induced surface reconstruction [1,39]).

The electronic structure of the clean W(001) as well as H-covered W(001) surface has been extensively studied by various experimental techniques and first-principles calculations [1,25,43-45]. However, calculated surface bands are not always consistent with UPES results, as they do for H/Mo(001) [32,46]. This discrepancy might be explained either by important role of relativistic effects (in particular, spin-orbit coupling) and many-body interactions, not properly accounted for in usual calculations (in other words, by the deficiency of the calculations), or to the restricted accuracy of the measurements of the energies of surface bands in early UPES studies.

The topology of Fermi surface plays important role not only in possible surface reconstructions, but also in the indirect interaction between adsorbed atoms (see, e.g., [18,47-49] for review). The *Umklapp* processes involving bulk and surface sheets of Fermi surface were reported to be responsible

also for the surface reflection coefficients for conducting electrons, which results in peculiarities of magnetoresistance of thin W(011) slabs at low temperatures [50]. Similar behavior was observed also for W(001) [51], and it is instructive therefore to calculate the Fermi surface of W(001) (we are not aware of any such calculations), of which the knowledge is ultimately important for interpretation of obtained experimental results.

## 2. Method

In the present study, fully relativistic DFT calculations (that is, with account for the spin-orbit coupling) were carried out with the ABINIT code [52] with LDA [53] exchange-correlation and Hartwigsen-Goedecker-Hutter (HGH) [54] norm-conserving pseudopotentials. The electronic structure of the surface was computed using the supercell (repeated slab) model with the vacuum gap about 12 Å. The slabs were built of 7 layers of W(001) atomic planes. Hydrogen adsorption was modeled by H monolayers on both sides of the W(001) slabs. The standard structural optimization was performed in all cases until the forces on atoms became below 0.05 eV/Å, which allowed for the determination of atomic positions with accuracy of ~0.02 Å. The 6×6×1 Monkhorst-Pack [55] lattice of k-points (including Γ point) and the energy cutoff of 20 Ha provided the $10^{-4}$ Ha convergence of total energy. For the (√2×√2)R45º structure, similar convergence was obtained with the 4×4×1 lattice. In the calculations of the Fermi surfaces, which require a dense k-point lattice for adequate displaying with XCrySDen [56], the 6×6×2 grid, giving 32 non-equivalent k points, was adopted. Surface weights for every band and k-point were estimated by the integration of the partial local electron density within atomic spheres (with r = 2.5 Bohr). The symmetry of the surface bands was determined from the dominant partial weights of the states decomposed into spherical harmonics at the surface atoms. In the course of the structural optimization the calculations were performed in semirelativistic approximation (i.e. without spin-orbit coupling). The phonon band structures and densities of states were calculated using the linear response function method, implemented in ABINIT.

## 3. Results of calculations

### 3.1. Surface reconstruction

In first-principles calculations using the repeat-slab (supercell) method, the equilibrated structure is characterized by the total energy (per unit cell), estimated at formally zero temperature, so that the entropy term in the free energy is eliminated. In the widely used Broyden optimization scheme, an initial (assumed) structure is varied according to calculated Hellmann-Feynman forces acting on atoms thus attaining the minimum energy configuration. This procedure, however, does not guarantee that the system attains the ground state corresponding to the true minimum of the energy. This is because of possible existence of several configurations having local minimums separated by energy barriers, so that the system can be frozen in some metastable configuration.

For the W(001) surface, the (1×1) structure is apparently stable. In particular, the Broyden optimization leads to a relaxation of the surface (a decrease of the interlayer spacing), but not to a reconstruction. Perhaps, for this reason it has been implicitly presumed that the (1×1) structure is an original configuration (if not the ground state) of the surface, which, for one or another reason, on cooling reconstructs to the (√2×√2)R45º structure (Fig. 1a). To reveal the driving force for the reconstruction, we have performed DFT calculations of total energies for 7-layer W(001) slabs with the (1×1) and (√2×√2)R45º structures of the surface layers.

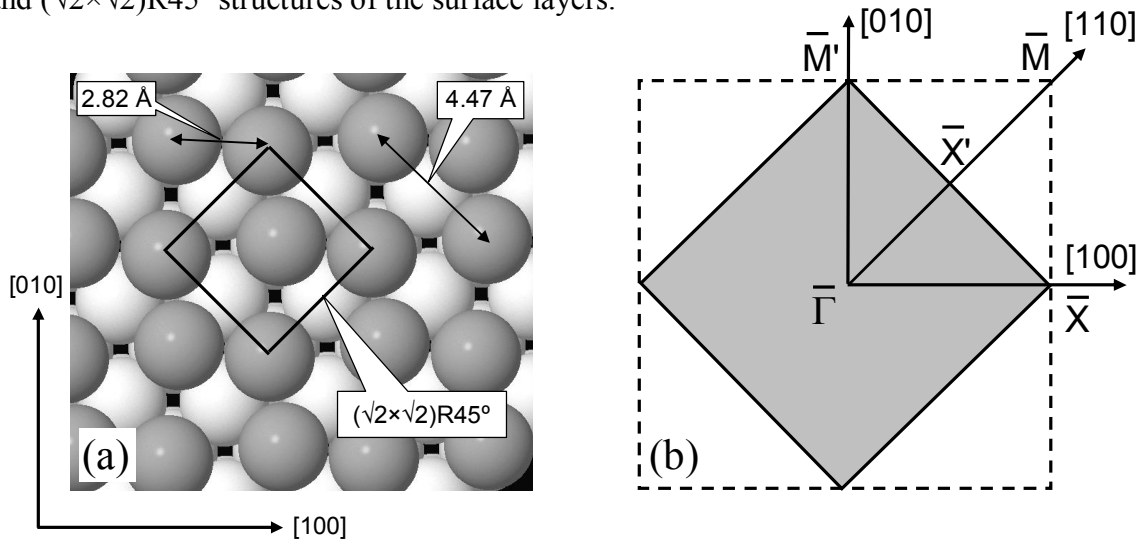


**Fig. 1.** (a): The (√2×√2)R45º structure of the reconstructed W(001) surface. The (√2×√2)R45º unit cell is shown by a solid square. (b): The surface Brillouin zone (BZ) for the (√2×√2)R45º structure is shown by a shadowed solid square; the dashed square indicates the BZ for the (1×1) structure.

When the surface atoms are slightly (by ~0.01 Å) shifted from the symmetric positions, which they occupy in the (1×1) structure, to avoid the symmetry constraint, the induced interatomic forces tend to further increase the shifts, and the structural optimization results in the formation of the

(√2×√2)R45º zigzag chains structure, in perfect agreement with the model suggested by Debe and King [3]. The most important result of these total energy calculations is that the (√2×√2)R45º structure of the surface indeed is favorable with respect to the (1×1) structure. The relative shifts of surface atoms (6.6 %) and the energy difference between the states (0.14 ±0.01 eV per atom) agree well with earlier LAPW estimates (110 meV [35]). However, in contrast to suggestions in Ref. [35], we have found a significant relaxation (the 12.7 % decrease of the interlayer spacing, which is twice the value reported in [35]) also for the (√2×√2)R45º reconstructed surface, which is consistent with *IV*-LEED data [5-10].

### 3.2. Surface states and resonances

The band structure and DOS of the (1×1) W(001) surface, calculated for the 7-layer slab after the structural optimization (that is, for relaxed surface), are shown in Fig. 2. The calculated surface bands (marked by symbols) agree well with earlier LAPW results [27,44] and UPES data [20,21,29,30]. There is a pronounced difference between the band structures calculated with and without account for spin-orbit coupling, in particular, in vicinity of $E_F$. Due to the spin-orbit coupling, the bands tend to split thus decreasing the density of states (DOS) at $E_F$, which results in the related decrease of the total energy.

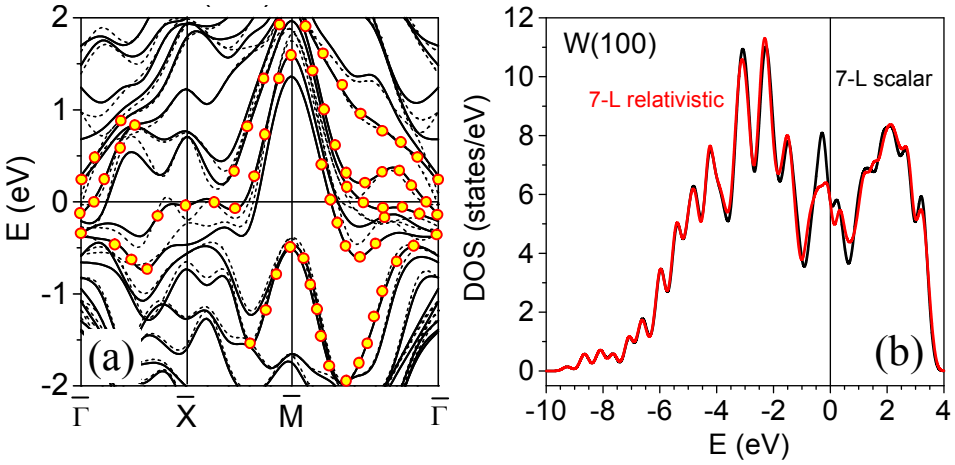


**Fig. 2.** The band structure (a) and DOS (b) of the (1×1) W(001) surface. Bands with strong surface weights are marked by symbols.

For the (√2×√2)R45º reconstructed surface, the Γ – M' direction in the BZ (which is the [110] crystallographic direction) corresponds to the Γ – X direction of the (1×1) surface lattice (see Fig. 1 b), so that it is instructive to compare the band structures of the reconstructed and non-reconstructed surfaces just along this direction to detect the difference induced by the reconstruction. The band structures along Γ – M' for the (√2×√2)R45º reconstructed W(001) surface and along Γ – X direction

for the (1×1) surface, calculated for optimized 7-layer slabs, are shown in Fig. 3. It is evident that the surface bands are pushed out from the vicinity of Fermi level, which is clearly indicated by the pronounced decrease in local density of states (LDOS) on the surface atom in this energy region (Fig. 3c).

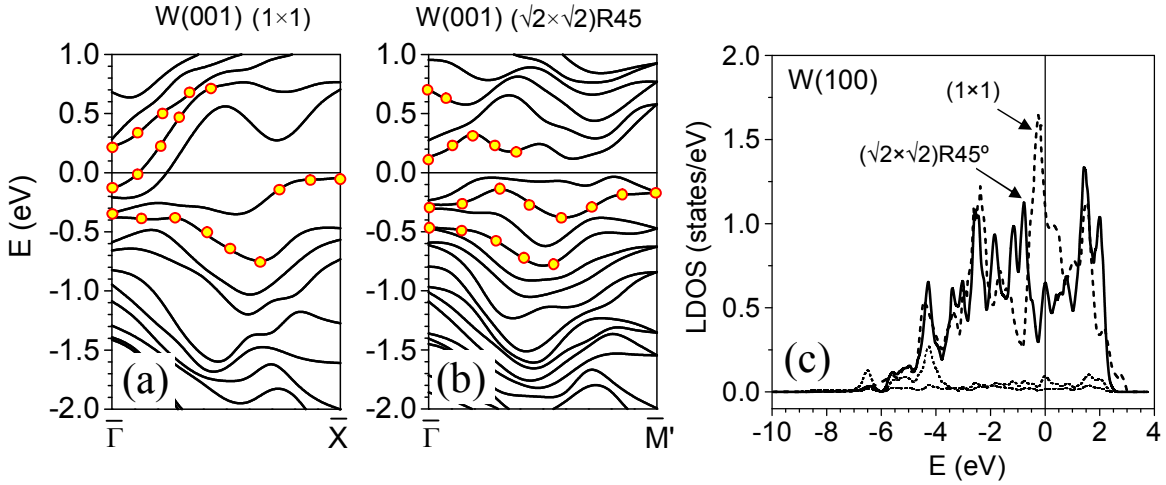


**Fig. 3.** The band structures for the (1×1) (a) and (√2×√2)R45º (b) W(001) surfaces and local density of states (LDOS) (c) on the surface atom.

Hence, the (√2×√2)R45º reconstruction of the W(001) surface leads to the decrease of the number of electrons at $E_F$, which results in the decrease of the electronic part of the total energy and might be considered opening a pseudo gap in the surface band structure. Although the SOC somewhat decreases the DOS at $E_F$, the overall effect on the electronic structure is found to be of marginal importance, so that the pointed discrepancy between calculated and UPES-derived surface bands [29,30] hardly could be explained by relativistic effects.

### 3.3. Hydrogen-induced changes of the electronic structure and phonon modes for c(1×1) H/W(001)

It is well established that H, at θ = 0.5, forms the c(2×2) structure, or, more rigorously speaking, shows the c(2×2) LEED pattern, similar to that of the (√2×√2)R45º reconstructed W(001) surface. Present DFT calculations, in agreement with earlier studies [44], suggest that H atoms are preferably adsorbed in bridge sites on W(001) for all coverages up to the complete physical monolayer (θ = 2.0). The H adsorption initiates redistribution of surface electronic density and density of states, which affects interatomic interactions. In other words, consistent with earlier findings [1,5,39,43-45], our results suggest that H, at θ = 0.5, tend to stabilize the c(2×2) structure, which therefore can be observed by LEED also at room temperature.

With increasing H coverage, changes in the surface electronic structure become well pronounced. The band structure and DOS of the c(1×1)-H/W(001) surface are shown in Fig. 4. Due to forming H – W bonds, the surface states are shifted down (away from the Fermi level). Consequently, the H adsorption eliminates the driving force for the surface reconstruction, since the electronic energy cannot be further reduced by means of the transformation of the surface states and related redistribution of electrons at the surface. This suggestion is directly confirmed by results of performed calculations of total energies for the unreconstructed (1×1) and (√2×√2)R45° reconstructed H-covered W(001) surfaces. Thus, in contrast to a clean W(001), the (1×1) structure of the 2H/W(001) surface is found to be stable and favored with respect to the reconstructed surface.

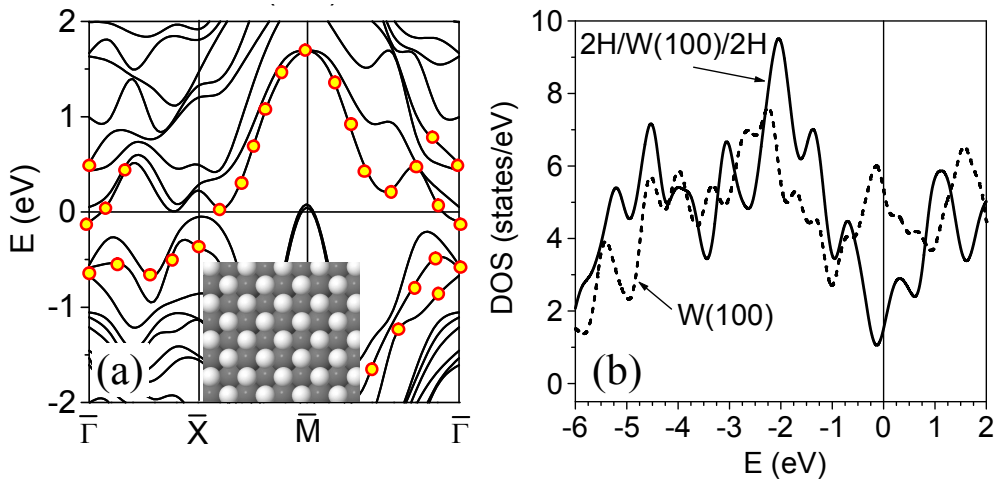


**Fig. 4.** The band structure (a) and DOS (b) for the c(1×1) H structure on W(001) surface at θ = 2.0.

The stability of a system can be studied also by means of calculations of phonon bands. When the structure occurs unstable, the related phonon mode becomes imaginary thus having negative $\omega^2$ values for corresponding directions in BZ (by convention, such bands are plotted with negative ω). Hence, by the presence or absence of phonon bands with negative ω – so-called soft modes – it is possible to conclude whether the structure is stable or not.

The phonon band structure, calculated for 5-layer W(001) slab with an unreconstructed (but relaxed and carefully optimized) (1×1) surface, is shown in Fig. 5 a. It is the soft mode in the Γ – M direction that initiates the reconstruction of the clean W(001) surface. In contrast, there are no any soft modes for the same slab but covered by hydrogen monolayers from both sides (Fig. 5 b), which clearly indicates the stability of the surface.

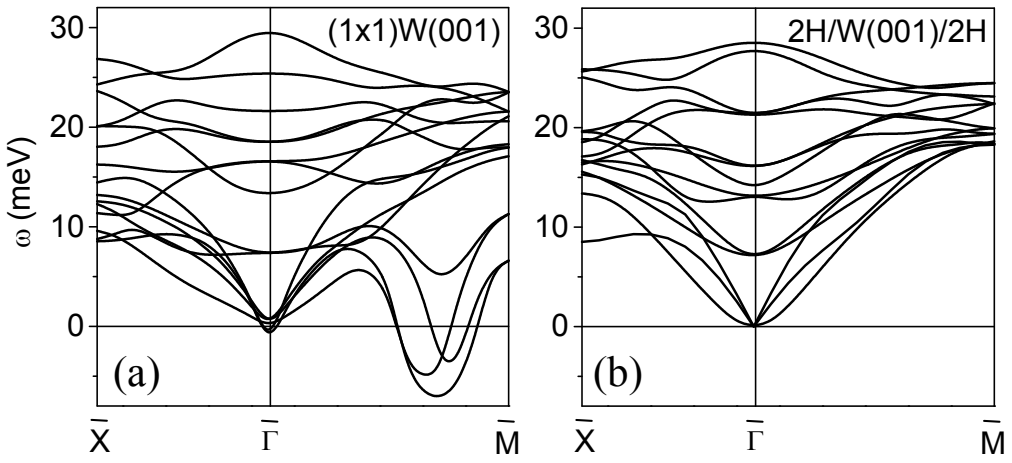


**Fig. 5.** The phonon band structure for the W(001) surface (a) and c(1×1) H/W(001) (b).

It should be noted that the actual shape of a calculated Fermi surface, plotted with the help of XCrysDen software [56], depends on peculiarities of interpolation scheme, on the number of k-points and degree of smoothing. (In some cases, in particular, for strongly anisotropic furrowed surfaces (like (112) of W and Mo), definitely flat segments of the Fermi surface indeed were obtained [16,17]). However, for the (1×1) W(001) 7-layer slab, the estimated Fermi surface (Fig. 6 a) does not demonstrate apparently flat segments which could provide any significant nesting, required for the Peierls-type CDW-induced reconstruction.

As discussed above, hydrogen adsorption removes surface bands away from the Fermi level, and therefore the Fermi surface becomes much simpler (Fig. 6 b). This result is of a primary importance for interpretation of the experiments on reflections of conductance electrons, because explains the decrease of the magnetoresistance of the W(001) surface under monolayer hydrogen as the result of the elimination of the channels of *Umklapp* processes involving surface sheets of the Fermi surface [50].

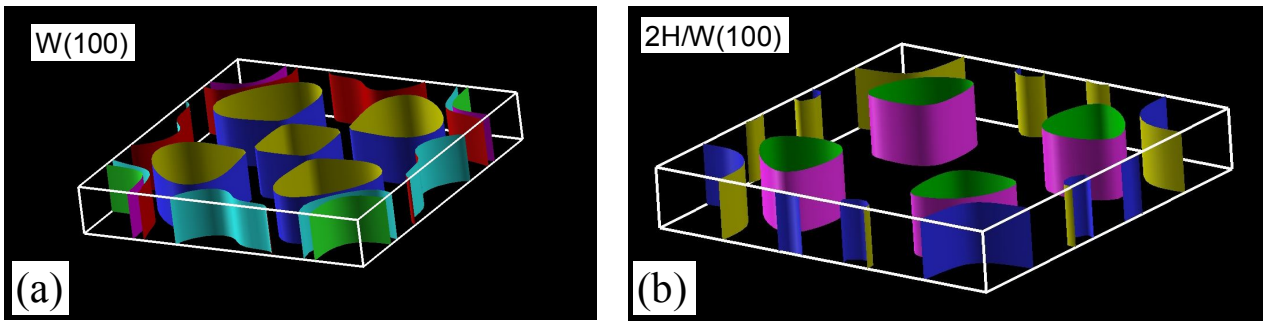


**Fig. 6.** The Fermi surfaces for the (1×1) W(001) (a) and c(1×1) H/W(001) (b).

## 4. Discussion: The driving force for surface reconstruction

### 4.1. Peierls transition

Present calculations, in particular, of the Fermi surface of W(001), do not support the concept of the Peierls'-type CDW-induced reconstruction of the W(001) surface [11-13,24]. Rather, they support the view that the CDW mechanism alone cannot be the driving force of the reconstruction [12,22]. As suggested by Johanness and Mazin [22], the "electronic" gain in energy is insufficient for a reconstruction and therefore in all cases, to accomplish the phase transition, certain lattice distortions must occur simultaneously with the forming CDW (in other words, the lattice distortions are not a result of CDW, but are equally important for the surface reconstruction). To illustrate the minor importance of CDW, Johanness and Mazin [22] performed model calculations for 1D chain of Na atoms, which is a classical example of the Peierls system. The result was confusing – though an artificial coupling of Na atoms indeed opened the band gap (the Peierls transition), the increased total energy effected returning forces, which, in the course of the "cold" structural optimization, restored the uniform interatomic spacing and hence a metallic state of the chain.

Because of importance of this result for understanding of the driving force for surface reconstruction, we also carried out such model DFT-LDA calculations for 1D Na chain. Following Johanness and Mazin [22], we started with the chain of equally spaced atoms with optimized lattice period (which was found to be of 3.22 Å, by 12% less than the nearest-neighbor distance in bcc Na, 3.66 Å). As expected, the Na chain was metallic with Fermi level at the middle of the band. Then the chain was slightly distorted, so that the distances between neighboring atoms were alternatively changed thus providing the doubling of the unit cell (so that the period of the cell became 6.44 Å). As the result of the periodic distortion, the band gap opened and the chain became semiconducting. However, consistent with findings in Ref. [22], the induced returning forces tend to restore the uniform spacing between Na atoms and hence restore the metallic state.

At the first glance, these model results discard the idea of Peierls transition (we do not consider here transversal shifts of atoms, which are known incapable to lift degeneracy – so called "gapless Peierls transition" [57-59]). This is not true, however, and the key is in the starting point of the simulations. Indeed, the initial structural optimization puts the atoms at the distances, for which the total energy (including electronic energy and Coulomb interactions between ion cores) is minimal and interatomic forces are zero. Then, if the distance between two atom decreases, the repulsion between them increases dramatically (though this is not the result of the so-called "Pauli repulsion", but, rather just a Coulomb interaction between ion cores, see Ref. [59] for more detailed discussion). This quickly increasing lateral repulsion (due to a steep rise of the potential energy for distances less than the

optimal) leads to a fast increase of the total energy, which cannot be compensated by the gain of electron energy due to forming CDW and related opening of the band gap.

Hence, the Peierls transition can occur only when the gain in the electronic energy due to forming CDW exceeds the loss of energy caused by enhanced Coulomb repulsion between ion cores at decreased interatomic distances. This is possible in the case when the average interatomic distance exceeds the equilibrium (optimal) distance in the chain, so that the repulsion between neighboring atoms caused by a decrease of the interatomic distance will be insignificant. (Recall that in one-electron picture, the chain of uniformly spaced Na atoms is metallic regardless the lattice period, which the puzzle inspired Mott to advance the theory of nonmetal-to-metal transitions).

Results of the model calculations of the band structure for the Na atomic chain with the (double) lattice period increased to 7.32 Å (which is twice the nearest-neighbor distance in bcc Na) are shown in Fig. 7. For the chain of uniformly spaced atoms, Fermi level crossing indicated a metallic state (Fig. 7a). However, this state is unstable with regard to Peierls distortion: the alternating coupling of atoms results in a decrease of total energy and related opening of the gap (Fig. 7b).

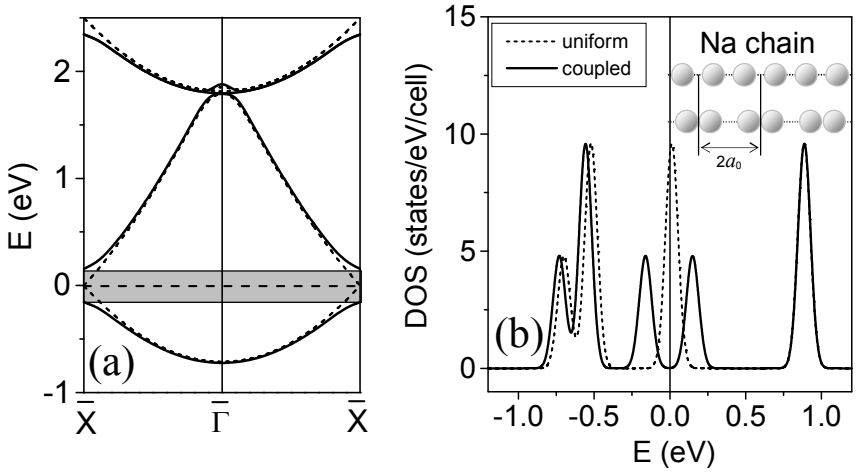


**Fig. 7.** The band structure (a) and DOS (b) for the 1D Na chain for $2a_0$ = 7.32 Å.

We underscore that now the lowering of the total energy is caused by the gain provided both by the redistribution of electrons and by the interaction of the ion cores. Hence, even in the classical model of the 1D Na chain, the driving force for the Peierls transition is not purely electronic, but unavoidably involves interatomic interactions, which initiate the lattice distortion. The interatomic interaction, obviously, depends on the electronic density distribution (including both Coulomb and exchange-correlation terms), so that the minimum of the potential of interatomic interaction has essentially electronic origin, and the "electronic" and "atomic" inputs into surface reconstruction hardly could be separated.

### 4.2. The ground state and interatomic interaction

The formation of the zigzag chains of the (√2×√2)R45º structure of W(001) surface can be explained in terms of interactions between neighboring W atoms. Indeed, a closer look onto the optimized surface structure (Fig. 8) allows one to notice that the surface atoms tend to shift from symmetric positions to become closer to each other – the distance between W atoms in the chain is of 2.82 Å (compare to 3.16 Å lattice period of the (1×1) W(001) surface). Since the interaction between W atoms is obviously attractive, the decrease of the interatomic distances leads to the decrease of the total energy. Furthermore, the nearest neighbor to the shifted atom is the atom of the next to surface layer, and the distance between these atoms in the equilibrated (√2×√2)R45º structure of W(001) surface is of 2.47 Å, which is even smaller than the 2.74 Å nearest-neighbor distance in the bulk bcc W crystal. (Probably, this unusual decrease of interatomic spacing can be attributed to the redistribution of electronic densities of the surface atoms forming the bonds with neighboring atoms in zigzag chains).

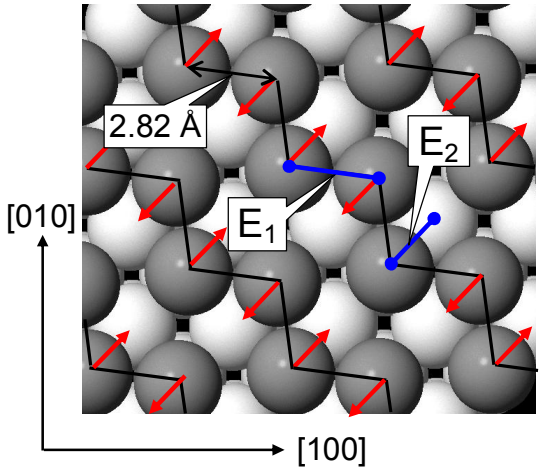


**Fig. 8.** The (√2×√2)R45º structure of W(001) surface. The shifts of the surface atoms (by 0.27 Å) are shown by arrows; zigzag lines were drawn to highlight the forming atomic chains. Due to the shifts, the atoms become closer to each other, thus forming bonds, and to the atoms of the next to surface layer. The related binding energies $E_1$ and $E_2$ serve as parameters in the Monte Carlo simulations.

The high symmetry of the (1×1) W(001) surface structure provoked its consideration as primary and therefore the formation of the (√2×√2)R45º structure as a result of a reconstruction of the surface. In fact, however, the situation is opposite. The surface atoms tend to occupy positions that provide the best available coordination (with respect to the bondlengths), which is accomplished in zigzag chains of the (√2×√2)R45º structure. Therefore, this structure of the surface correspond to the ground state of the system and there is no need to assume any kind of phase transition for its formation. In turn, with increasing temperature, the LEED pattern shows the transformation to the (1×1) surface structure, which may be viewed either as the second-order phase transition [5,11,13] or just as a simple melting,

giving not perfectly ordered surface layer, consistent with the behavior of W(001) suggested in Refs. [6,12, 22,25,34-36].

To support the short-range interaction view, we have carried out the Monte Carlo simulation of the formation and melting of the (√2×√2)R45º structure within the lattice gas model using Metropolis algorithm [60-64]. The top surface layer was treated as an adsorbed layer (with θ = 1), and W surface atoms could occupy either hollow sites or the sites corresponding to shifts from hollow sites in any of four {110} directions by 0.27 Å (as estimated from DFT calculations for optimized surface). The modeled segment of the surface contained 50×50 hollow sites, which, with 4 available shifts for every site, gives 12500 sites. The periodic boundary conditions were adopted.

Initially, W atoms were randomly shifted (with respect to the high-symmetry hollow sites) and then allowed to move either towards the hollow (for the shifted atoms) or, for the case of the atom in the hollow site, in randomly chosen one of four {110} directions. The probability of unfavorable moves was estimated according to Boltzmann statistic as $W = \exp(-\Delta E/k_B T)$, where $\Delta E$ is the increase of the total energy due to the move and $k_B$ is the Boltzmann constant. For favorable moves, i.e. those giving the gain in energy ($\Delta E < 0$), the probability was taken to be unity. After a sufficient number of such moves (usually about 100 per atom), the layer attains thermodynamic equilibrium (which corresponds to the minimum of the free energy). Then, the degree of ordering of the layer can be estimated from LEED patterns, calculated in the kinematical approximation [63-65].

The change of the total energy $\Delta E$ depends on the energies of lateral interactions and interaction with the next-to-surface atomic layer. The lateral interactions were accounted by means of the adjustable parameter $E_1$ that corresponds to the energy of attraction between the nearest neighbors in zigzag chain of the (√2×√2)R45º structure, and the interaction with the substrate atoms by parameter $E_2$ that determines the gain in energy due to the shifts of surface atoms from the hole sites and related bonding with the nearest subsurface atom (see Fig. 8). The gain of the total energy due to the surface reconstruction, obtained from the DFT calculations (see Section 3.1), is of 0.14 ±0.01 eV per atom, so that it is reasonable to chose initial values of the energy parameters to obey the relation $E_1 + E_2 = -0.14$ eV. The results of the Monte Carlo simulations with $E_1 = -0.11$ eV and $E_2 = -0.03$ eV are shown in Figs. 9 and 10.

The snapshots and related LEED patterns, obtained for the model surface equilibrated at several characteristic temperatures, are shown in Fig. 9. At T = 300 K (Fig. 9 a), the surface layer is essentially disordered, and the LEED pattern corresponds to the (1×1) structure. With decreasing T, domains of the zigzag chains of the (√2×√2)R45º structure are formed, and in some cases their areas occur close to each other so that a well pronounced c(2×2) LEED pattern is observed. An example of such structure, formed at T = 240 K, is presented in Fig. 9 b. Finally, for the temperatures below transition temperature $T_c$, the structure becomes perfectly ordered with one prevailing orientation of zigzag chains, as illustrated in Fig. 9 c for the layer at T = 150 K. (For real surfaces, the LEED pattern will correspond to both orientations of large domains of zigzag chains thus showing the c(2×2) lattice).

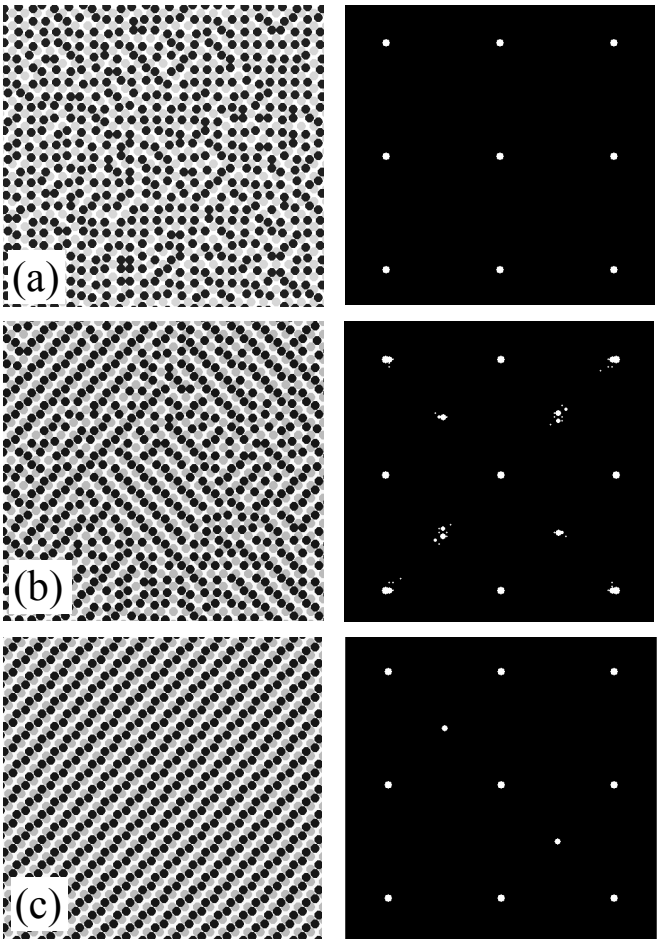


**Fig. 9.** The snapshots and related LEED patterns, obtained in the Monte Carlo simulations for the model surface equilibrated at several characteristic temperatures. (a): T = 300 K; the surface layer is essentially disordered, and the LEED pattern corresponds to the (1×1) structure. (b): T = 240 K; forming domains with two different orientations of zigzag chains give rise to a well pronounced c(2×2) LEED pattern. (c): T = 150 K; ordered (√2×√2)R45º structure with one predominant orientation of zigzag chains.

The order-disorder transition [61-64] in the surface layer can be characterized by the temperature dependence of the relative intensity of the (1/2,1/2) reflection, corresponding to the c(2×2) structure (Fig. 10). In the course of the simulations, the temperature was decreased stepwise from 350 K to 150 K with equilibration of the structure at each step of 10 K. The transition temperature was estimated from the middle point of the slope, that is, corresponding to the value at which relative intensity of the

reflection is of 0.5. The obtained dependence and transition temperature $T_c$ = 240 K agree well with LEED data reported by Debe and King [3], shown in Fig. 10 by a dashed line.

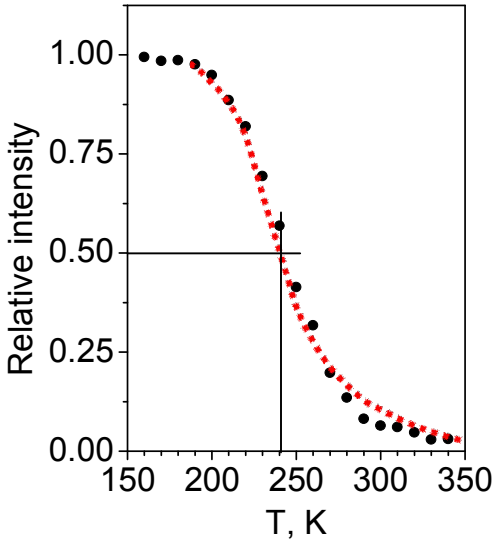


**Fig. 10.** The temperature dependence of the relative intensity of the (1/2,1/2) reflection, corresponding to the c(2×2) structure, obtained in Monte Carlo simulations (black dots). Temperature was decreased stepwise from 350 K to 150 K with equilibration of the structure at each step of 10 K. The transition temperature was estimated as corresponding to the 0.5 relative intensity of the reflection. LEED data by Debe and King [3] are shown by a dashed line.

## 5. Conclusion

A surface does not have to reproduce the bulk structure, and the W(001) surface is an example of such case. It is only a quite natural intention to present the surface structure in a simple way that provokes the explanation of the (√2×√2)R45° structure as a reconstructed W(001) surface, so that this reconstruction from the (1×1) structure requires one or another exotic mechanism such as CDW Peierls-like or Jan-Teller with softening phonon modes. Adsorbed physical monolayer of hydrogen stabilizes the (1×1) structure of the H/W(001) surface because of the redistribution of the surface electronic states. Specifically, due to forming adsorption bonds, the surface bands of W(001) shift downwards in energy so that the DOS at $E_F$ significantly decreases. Consequently, any surface reconstruction would not be able to effect a substantial further decrease of the electronic energy, and therefore the H-covered W(001) surface is stable.

While there are important differences between electronic structures of the W(001) with (1×1) and (√2×√2)R45° surface structures, in particular, at Fermi level, the shape of the Fermi surface for the (1×1) W(001) has little relevance to the formation of the (√2×√2)R45° surface structure. In contrast, as follows from the present calculations, the reduced electronic part of the total energy results in the total energy decrease with respect to that for the (1×1) surface and therefore it is not the (1×1) but the (√2×√2)R45° surface structure that presents the ground state of the system. Hence, the formation of the

($\sqrt{2}\times\sqrt{2}$)R45º surface structure of W(001) is natural and does not require any special mechanism to be accomplished.

With increasing temperature, the surface layer demonstrates the order-disorder transition, which may be viewed as melting, or the first-order phase transition, so that the (1×1) LEED pattern, observed at room temperature, corresponds to essentially disordered surface layer. The dependence of the relative intensity of the characteristic LEED reflection on temperature, obtained with the help of Monte Carlo simulations using the interaction energies estimated from DFT calculations, is in good agreement with available experimental data, thus supporting the concept of the order-disorder type of the transition between the low-temperature ($\sqrt{2}\times\sqrt{2}$)R45º and room-temperature (1×1) surface structures of W(001).

**References**


1. K. Yonehara and L. F. Schmidt, Surf. Sci. **25**, 238 (1971).
2. T. E. Felter, R.A. Barker, and P. J. Estrup, Phys. Rev. Lett. **38**, 1138 (1977).
3. M.K. Debe and D.A. King, Phys, Rev. Lett. **39**, 708 (1977); J. Phys. C: Solid State Phys. **10**, L303 (1977).
4. A. J. Melmed, S. T. Ceyer, R. T. Tung, and W. R. Graham, Surf. Sci. **111**, L701 (1981)
5. M. K. Debe and D. A. King, Surf. Sci. **81**, 193 (1979).
6. J. C. Campuzano, J. E. Inglesfield, D. A. King, and C. Somerton, J. Phys. C: Solid State Phys. **14**, 3099 (1981).
7. J. A. Walker, M. K. Debe, and D. A. King, Surf. Sci. **104**, 405 (1981).
8. F. S. Marsh, M. K. Debe, and D. A. King, J. Phys. C: Solid State Phys. **13**, 2799 (1980).
9. G. Schmidt, H. Zagel, H. Landskron, K. Heinz, K. Müller, and J. B. Pendry, Surf. Sci. **271**, 416 (1992).
10. H. Landskron, N. Bickel, K. Heinz, G. Schmidtlein, and K. Müller, J. Phys.: Condens. Matter **1**, 1 (1989).
11. E. Tosatti, Sol. St. Comm. **25**, 637 (1978).
12. J. E. Inglesfield, Vacuum **31**, 663 (1981); Prog. Surf. Sci. **20**, 105 (1985).
13. D. A. King, Physica Scripta **4**, 34 (1983).
14. T. Aruga, J. Phys.: Condens. Matter **14**, 8393 (2002).
15. X. W. Wang and W. Weber, Phys. Rev. Lett. **58**, 1452 (1987).
16. A. Fasolino and E. Tosatti, Phys. Rev. B **35**, 4264 (1987).
17. K. Fukutani, H. Hayashi, I. N. Yakovkin, T. R. Paudel1, T. Habuchi, D. Hirayama, J. Jiang, H. Iwasawa, K. Shimada, N. Wu, E. Y. Tsymbal1, Ya. B. Losovyj, and P. A. Dowben, Phys. Rev. B **85**, 155435 (2012).
18. I. N. Yakovkin, K. Fukutani, H. Hayashi, J. Jiang, T. Horike, Y. Nagata, T. Habuchi, D. Hirayama, H. Iwasawa, K. Shimada, Ya. B. Losovyj and P. A. Dowben, Phys. Rev. B **86**, 125401 (2012).
19. Ya. B. Losovyj, I. N. Yakovkin, H.-K. Jeong, and P. A. Dowben, Phys. Stat. Sol.(b) **241**, 829 (2004).
20. J. C. Campuzano, D. A. King, C. Somerton, and J. E. Inglesfield, Phys. Rev. Lett. **45**, 1649 (1980).
21. J. C. Campuzano, J. E. Inglesfield, D. A. King, and C. Somerton, J. Phys. C: Solid State Phys. **14**, 3099 (1981).

22. M. D. Johannes, I. I. Mazin, Phys. Rev. B **77**, 165135 (2008).
23. J. E. Inglesfield, J. Phys. C **12**, 149 (1979).
24. I. Terakura, K. Terakura, and N. Hamada, Surf. Sci. **103**, 103 (1981).
25. L. D. Roelofs and S. C. Ying, Surf. Sci. **147**, 203 (1984).
26. H. Krakauer, M. Posternak, and A. J. Freeman, Phys. Rev. Lett. **43**, 1885 (1979).
27. M. Posternak, H. Krakauer, A. J. Freeman, and D. D. Koelling, Phys. Rev. B **21,** 5601 (1980).
28. L. F. Mattheiss and D. R. Hamann, Phys. Rev. B **29**, 5372 (1984).
29. K. E. Smith, G. S. Elliott, and S. D. Kevan, Phys. Rev. B **42**, 5385 (1990).
30. G. S. Elliott, K. E. Smith, and S. D. Kevan, Phys. Rev. B **44**, 10826 (1991).
31. K. E. Smith and S. D. Kevan, Phys. Rev. B **43**, 3986 (1991).
32. K. E. Smith and S. D. Kevan, Phys. Rev. B **45**, 13642 (1992).
33. J.W. Chung, K.S. Shin, D.H. Baek, C.Y. Kim, H.W. Kim, S.K. Lee, C.Y. Park, S.C. Hong, T. Kinoshita, M. Watanabe, A. Kakizaki, and T. Ishii, Phys. Rev. Lett. **69**, 2228 (1992).
34. D. Singh and H. Krakauer, Phys. Rev. B **37**, 3999 ( 1988).
35. R. Yu, H. Krakauer, and D. Singh, Phys. Rev. B **45**, 8671 (1992).
36. C. L. Fu, A. J. Freeman, E. Wimmer, and M. Weinert, Phys. Rev. Lett. **54**, 2261 (1985).
37. W. K. Han, and S. C. Ying, Phys. Rev. B 41, 9163 (1990).
38. L. N. Ryabchikov, Ukr. Fiz. Zh. **9**, 293 (1964).
39. P. J. Estrup and J. Anderson, J. Chem. Phys. **45**, 2254 (1966).
40. V. J. Mimeault and R. S. Hansen, J. Chem. Phys. **45**, 2240 (1966).
41. J. A. White, D. M. Bird, and M. C. Payne, Phys. Rev. B **53**, 1667 (1996).
42. Yu. G. Ptushinskii, Low Temp. Phys. **30**, 1 (2004).
43. N. V. Smith and L. F. Mattheiss, Phys. Rev. Lett. **37**, 1494 (1976).
44. M. Weinert, A. J. Freeman, and S. Ohnishi, Phys. Rev. Lett. **56**, 2295 (1986).
45. K. E. Smith and S. D. Kevan, Phys. Rev. Lett. **64**, 567 (1990).
46. K. E. Smith and S. D. Kevan, Phys. Rev. B **43**, 1831 (1991).
47. T. T. Tsong, Phys. Rev. B **6**, 417 (1972).
48. T. L. Einstein, CRC Crit. Rev. Sol. St. and Mat. Sci. **7**, 261 (1978).
49. O. M. Braun and V.K. Medvedev, Sov. Phys. Usp. **32**, 328 (1989).
50. O. A. Panchenko and S. V. Sologub, Phys. Rev. B **71**, 193401 (2005).
51. P. P. Lutsishin, O. A. Panchenko, and S. V. Sologub, Poverkhnost' **11**, 69 (2001).

52. X. Gonze, J.-M. Beuken, R. Caracas, F. Detraux, M. Fuchs, G.-M. Rignanese, L. Sindic, M. Verstraete, G. Zerah, F. Jollet, M. Torrent, A. Roy, M. Mikami, Ph. Ghosez, J.-Y. Raty, and D.C. Allan, Comput. Mat. Sci. **25,** 478 (2002).
53. S. Goedecker, M. Teter, and J. Hutter, Phys. Rev. B **54**, 1703 (1996).
54. C. Hartwigsen, S. Goedecker, and J. Hutter, Phys. Rev. B **58**, 3641 (1998).
55. H. J. Monkhorst and J. D. Pack, Phys. Rev. B **13**, 5188 (1976).
56. A. Kokalj, J. Molecular Graphics and Modelling **17 (3)**, 176 (1999).
57. I. P. Batra, Gapless Peierls transition, Phys. Rev. B **42**, 9162 (1990).
58. I. N. Yakovkin, Appl. Surf. Sci. **252**, 6127 (2006).
59. I. N. Yakovkin, Crystals **6**, 143 **(**2016).
60. N. Metropolis, A. W. Rosenbluth, M. N. Rosenbluth, A. H. Teller, and E. Teller. J. Chem. Phys. **21**, 1087 (1953).
61. T. T. Tsong, Surf. Sci. **122**, 99 (1982).
62. I. N. Yakovkin, Surf. Sci. **282**, 195 (1993); Surf. Sci. **559/1**, 29 (2004).
63. N. V. Petrova and I. N. Yakovkin, Surf. Sci. **578/1-3**, 162 (2005).
64. R. Szukiewicz, J. Kołaczkiewicz, and I. N. Yakovkin, Surf. Sci. **602**, 2610 (2008).
65. Ivan Yakovkin, Jr., Proc. XII International Conference "Electronics and Applied Physics", October 19-22, 2016, Kyiv, Ukraine, p. 96.